Flow through Negatively Charged, Nanoporous Membranes Separates Li+ and K+ due to Induced Electromigration

Journal:	*ChemComm*
Manuscript ID	CC-COM-04-2020-003143.R2
Article Type:	Communication

COMMUNICATION

Flow through Negatively Charged, Nanoporous Membranes Separates Li^+ and K^+ due to Induced Electromigration

Received 00th January 20xx,
Accepted 00th January 20xx

DOI: 10.1039/x0xx00000x

Chao Tang, [a] Andriy Yaroshchuk,[b,c] and Merlin L. Bruening *[a,d]

Flow through negatively charged nanopores separates Li^+ and K^+ with selectivities up to 70 and Li^+ passages from 20% to above 100%. Remarkably, both the Li^+/K^+ selectivity and Li^+ passage initially increase with flow rate, breaking the permeability/selectivity trade-off. Modelling demonstrates that flow through the membranes creates electric fields that retard transport of cations. Selectivity increases with flow rate because the K^+ electromigration velocity exceeds its convective velocity, but for Li^+ electromigration is weaker than convection. Modelling also shows the importance of controlling concentration polarization. With further work, related separations might provide highly pure Li salts for battery manufacturing.

Ion separations are vital in providing pure compounds used in fabricating for fabricating batteries,[1] catalysts,[2] magnets,[2] and electronic devices.[3] Conventional salt purification methods such as precipitation, crystallization, solvent extraction, ion-exchange, and electroplating are effective. However, challenges remain in increasing yields, decreasing separation times, and differentiating among similar ions.[2, 4] Membrane processes can potentially provide continuous separations for purifying salts, particularly at low concentrations. Nanofiltration membranes, for example, show high selectivities between monovalent and divalent ions, largely due to exclusion of divalent species.[5] Unfortunately, selective exclusion usually does not separate ions with the same charge.

Recent studies show monovalent ion separations based on differences in ion hydrated radii or specific interactions with membrane materials.[4, 6] However, this often requires exquisite control over the membrane structure as well as the use of very small membrane areas to avoid defects. In this work we show that simple flow through unmodified nanopores in negatively charged track-etched membranes (10 or 30 nm nominal pore diameters) leads to highly selective Li^+/K^+ separations without the need to carefully control the membrane chemistry. Most importantly, with increasing flow rate both selectivity and passage (defined as the ratio of permeate to feed concentration) of the desired ion increase simultaneously, whereas nearly all membrane separations show a trade-off between permeability (transport rate) and selectivity.[7] Below, we first give a qualitative picture of the separation mechanism and then present experimental and modelling data that demonstrate the high selectivities and passages that are possible when flowing salt solutions through nanoporous membranes.

Charged nanopores offer unique opportunities for ion separations because they exclude ions with the same charge sign as the pore surface. For a negatively charged surface this leads to an excess of mobile cations in the pore (Figure 1A). Due to the excess mobile cations, pressure-driven flow through these pores creates streaming potentials, where the pore outlet is positive (Figure 1B). The streaming potential causes electromigration of cations toward the pore inlet and of anions toward the outlet so the net anion velocities are much larger than those of the cations. The product of velocity and concentration

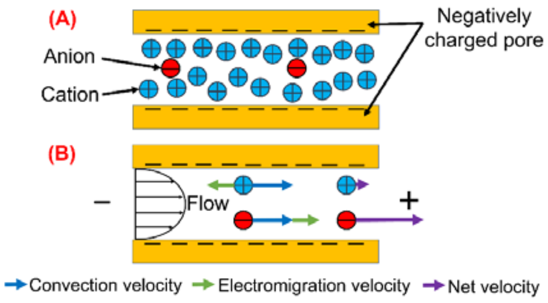

Figure 1. (A) Qualitative ion distribution in a negatively charged nanopore and (B) scheme of streaming potential and ion velocity components during flow through the pore. Due to anion exclusion, the anion velocity must be much larger than the cation velocity to maintain equal cation and anion fluxes (flux=concentration times velocity).

---

[a] *Department of Chemical and Biomolecular Engineering, University of Notre Dame, Notre Dame, IN,46656 USA*
[b] *Polytechnic University of Catalonia, av. Diagonal 647, 08028 Barcelona, Spain*
[c] *ICREA, pg.L.Companys 23, 08010 Barcelona, Spain, Barcelona, Spain*
[d] *Department of Chemistry and Biochemistry, University of Notre Dame, Notre Dame, Indiana 46556, United States*
* Corresponding author. Email: mbruenin@nd.edu orcid.org/0000-0002-6364-6840

Electronic Supplementary Information (ESI) available: experimental methods, scanning electron microscopy images, experimental data, modelling rationale, modelling results, and glossary and symbols. See DOI: 10.1039/x0xx00000x

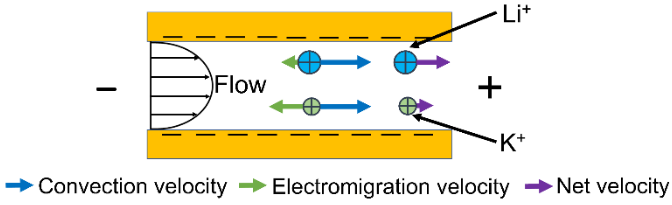

Figure 2. Scheme of Li$^+$/K$^+$ separation during flow through a negatively charged nanopore. Electromigration (green arrows) retards K$^+$ more than Li$^+$ due the higher mobility of K$^+$, whereas the convective velocities of both ions (blue arrows) are the same.

is the same for cations and anions, so their fluxes are the same and there is no current (Figure 1B).

When a solution contains two cationic species with different electrophoretic mobilities, for example K$^+$ and Li$^+$, the streaming potential opposes the convective transport to different extents for each ion, and this leads to Li$^+$/K$^+$ separations. Li$^+$ has a larger hydrated radius than K$^+$[8] so the electrophoretic mobility (and hence the electrophoretic velocity) of K$^+$ is nearly twice that for Li$^+$.[9] Thus, in mixtures of these ions electromigration retards K$^+$ transport more than Li$^+$ transport (Figure 2). In contrast, the velocity due to convection (flow) is the same for all ions. As a result, K$^+$ moves through the negatively charged nanopore at a slower rate than Li$^+$.

Importantly, when the K$^+$ electromigration velocity exceeds its convective velocity (whereas for Li$^+$ electromigration remains weaker than convection), selectivity becomes very high due to the low passage of K$^+$. Under these conditions, as the flow rate increases, the electromigration flux component compensates the sum of convection and diffusion flux components, and the K$^+$ passage should approach zero.[10] As a result, the Li$^+$/K$^+$ selectivity increases dramatically as the flow rate (or transmembrane pressure) rises.

A few papers presented this separation mechanism and demonstrated selectivities around 10 or less with either membranes that contained heterogeneous pores or membrane cells with insufficient transmembrane pressure or stirring.[11] This work employs polycarbonate track-etched membranes containing approximately cylindrical pores with nominal 30 or 10 nm diameters. We chose these membranes for four reasons. First, the nanopores are negatively charged at neutral or higher pH, likely due to the ionizable groups formed during the chemical etching that creates the pores.[12] Second, the 30 or 10 nm pores are small enough to give strong anion exclusion throughout the pore at low (0.2 to 1 mM) ionic strength. This exclusion leads to large streaming potentials that give rise to low K$^+$ transport and high Li$^+$/K$^+$ selectivities. Third, the pores are more than an order of magnitude larger than the hydrated ion radii, so they should not significantly change ion mobilities. Fourth, the pore diameters are large enough to allow sufficiently high flow rates under readily available transmembrane pressures. High flow rates are important for achieving large Li$^+$/K$^+$ selectivities. The supplementary information provides SEM images and physical properties of membranes (sections S1 and S2), along with estimation of pore sizes based on water flow (section S3.6). One disadvantage of these membranes is their fragility, but we developed a seal that does not damage the membranes under high pressures (supplementary material section S1.3).

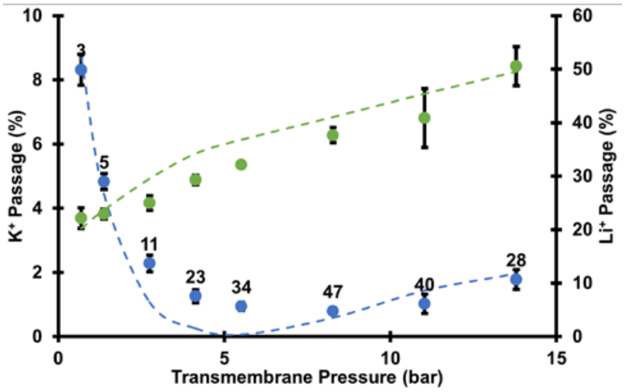

Figure 3. K$^+$ (blue, left y-axis) and Li$^+$ (green, right y-axis) passages during flow of a 0.1 mM KCl, 0.1 mM LiCl mixture through track-etched membranes (30 nm pores) using various transmembrane pressures. Dashed lines show simulation results with a linear combination of 10-µm (97%) and 75-µm (3%) unstirred layers. The simulation assumes a surface charge density of -3 mC/m^2. This charge density is consistent with stationary membrane potential measurements (see Section S3.5 of the supplementary information). The numbers above K$^+$ passages are Li$^+$/K$^+$ selectivities at the given pressure.

Figure 3 shows the Li$^+$ and K$^+$ passages and the Li$^+$/K$^+$ selectivities for various transmembrane pressures during flow of a 0.1 mM LiCl, 0.1 mM KCl mixture through a membrane with 30 nm pores. The Li$^+$/K$^+$ selectivity is simply the ratio of the ion permeate concentrations because their feed concentrations are equal. Notably the K$^+$ passage initially decreases dramatically with increasing pressure (flow rate is proportional to pressure), whereas the Li$^+$ passage monotonically increases. Thus, at low flow rates increasing the pressure overcomes the permeability/selectivity trade-off, which leads to a maximum selectivity of 47 at a pressure of 8.3 bar. At the highest flow rate (or pressure) in the figure, selectivity decreases to 28, presumably due to concentration polarization (see below).

The Li$^+$/K$^+$ separation relies on a negatively charged pore surface to exclude anions, and increasing the surface charge density should enhance selectivities (see section S5.6 of the supplementary information). A high solution pH may deprotonate surface functional groups to enhance the membrane charge. Thus, we also examined the Li$^+$/K$^+$ separation using a 0.1 mM LiOH, 0.1 mM KCl mixture (pH~10). As Figure 4 shows, under these conditions the Li$^+$/K$^+$ selectivity reaches 70. More importantly, both selectivity and Li$^+$ passage increase until the pressure exceeds 11 bar, overcoming the permeability/selectivity tradeoff.

The above experiments employ very dilute solutions to ensure that anion exclusion is strong, which limits the method applicability. Thus, we performed separations with somewhat more concentrated solutions (0.5 mM LiOH, 0.5 mM KCl), and the maximum selectivity decreased to around 20 (Figure S8). However, the Li$^+$ passage is high and even *exceeds 100%* at large flow rates, and a selectivity of 20 is still impressive. The high passage may allow multi-stage separations to efficiently produce highly pure Li$^+$.

We also examined separations with a 0.5 mM LiOH, 0.5 mM KCl mixture using membranes containing 10 nm pores and

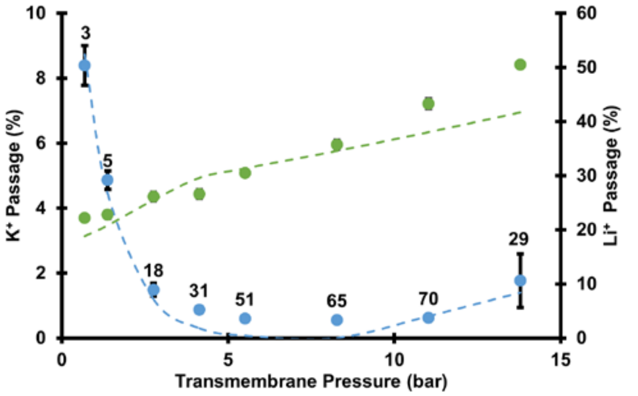

Figure 4. K$^+$ (blue, left y-axis) and Li$^+$ (green, right y-axis) passages during flow of a 0.1 mM KCl, 0.1 mM LiOH mixture through track-etched membranes (30 nm pores) using various transmembrane pressures. Dashed lines show simulation results with a linear combination of 10-µm (97%) and 75-µm (3%) unstirred layers. The simulation assumes a surface charge density of -5 mC/m^2. The numbers above K$^+$ passages are Li$^+$/K$^+$ selectivities at the given pressure.

found a selectivity of 60 at a transmembrane pressure of 27.6 bar. The Li$^+$ passage is 45% under these conditions. (With 30 nm pores, the maximum selectivity is 20 with a Li$^+$ passage of 92%). The higher selectivity and lower Li$^+$ passage in the 10 nm pores correspond to stronger streaming potentials due to more anion exclusion. (At 1 mM ionic strength, the electrical double-layer overlap is nearly complete in 10 nm pores because the Debye length is ~10 nm, whereas overlap is less in 30 nm pores.) These results indicate that smaller pores will allow highly selective separations at higher concentrations. In the supplementary information (sections S5.5 and S5.6), we explore the effects of pore size and surface charge density on simulated Li$^+$/K$^+$ separations.

The experimental data in Figures 3-4 and S8 demonstrate that high Li$^+$/K$^+$ selectivities and Li$^+$ passages are simultaneously possible when flowing salt solutions through charged nanopores. However, understanding the trends for each ion in these figures requires modelling, particularly when concentration polarization (see below) is involved. In this work, we employ the extended Nernst-Planck equation, Eq(1),

$$j_i = -D_i \frac{dc_i}{dx} - z_i c_i \frac{D_i F}{RT}\frac{d\phi}{dx} + c_i j_v \qquad (1)$$

to describe transport in the unstirred layer, and a related equation to model ion flux in the membrane pores (see Section S4 of the supplementary information). In Eq(1), j_i, D_i, z_i, and c_i are the flux, diffusion coefficient, charge, and concentration of ion i, respectively. Additionally, ϕ is the electrostatic potential, j_v is the convective solution velocity, and F, R, and T are Faraday's constant, the gas constant, and temperature, respectively. The three terms on the right side of Eq(1) describe transport by diffusion, electromigration, and convection modes, respectively.[13]

Concentration polarization (CP). CP is the accumulation of rejected ions within an unstirred layer at the feed/membrane interface (Figure 5). This occurs when flow brings ions to the feed/membrane interface, and only a fraction of these ions passes through the membrane (passage is <100%). Ion accumulation in the unstirred layer increases with increasing flow rate (more ions come to the membrane surface), smaller ion passage (fewer ions go through the membrane), or less efficient stirring (thicker unstirred layers).

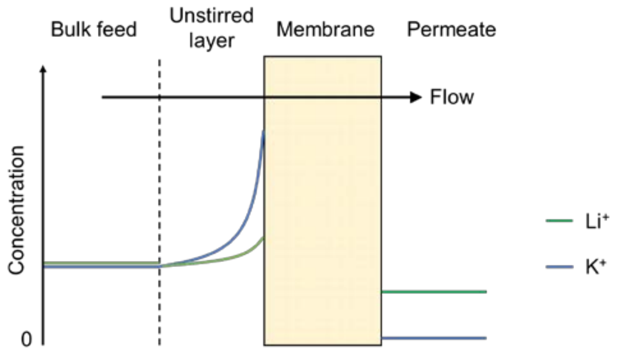

Figure 5. Qualitative K$^+$ (blue) and Li$^+$ (green) concentration profiles in the bulk feed, unstirred layer, and permeate. Rejected ions accumulate within the unstirred layer, and K$^+$ accumulates more than Li$^+$ because K$^+$ has a lower passage.

CP decreases the streaming potential for two reasons. First, the increase in ionic strength near the membrane surface weakens the anion exclusion within the negatively charged nanopores. The resulting increase in the anion concentration inside the pore decreases the streaming potential required to maintain zero current. Second, because of its lower passage K$^+$ should accumulate at the feed/membrane interface much more than Li$^+$. This gives rise to a higher K$^+$/Li$^+$ ratio in the pore as well as in the unstirred layer. The increased fraction of K$^+$ decreases the streaming potential because K$^+$ is more mobile than Li$^+$ and, thus, requires a smaller streaming potential to maintain zero current. In short, both reduced anion exclusion and higher K$^+$ content lower the streaming potential (relative to no CP, see section S5.1 in the supplementary information).

The Effect of CP on K$^+$ passages. In Figures 3-4 and S8, K$^+$ passage first decreases dramatically with increasing transmembrane pressure, then plateaus, and finally increases at the highest pressures. This trend stems from the interplay of the three modes of ion transport (diffusion, electromigration, and convection), as well as CP. Most importantly, with minimal CP, the magnitude of the K$^+$ electromigration velocity is greater than its convective velocity, and K$^+$ moves through the membrane due to diffusion. As pressure (or flow rate) increases, the sum of electromigration, diffusion, and convective flux components approaches zero, and this leads to decreases in K$^+$ passage with pressure. However, CP becomes more pronounced with increasing flow rate, and the decrease in streaming potential and accumulation of K$^+$ due to CP eventually lead to a K$^+$ electromigration velocity that is smaller than its convective velocity. This results in significant unwanted K$^+$ passage at the highest pressures.

We hypothesize that the increase in K$^+$ passage at the highest pressures in Figures 3-4 and S8 stems from a small region of the membrane area with less efficient stirring (modelled as a 75-µm unstirred layer). In such a region, CP would be especially pronounced so the local K$^+$ flux will be high. Heterogeneous unstirred layers are unavoidable in stirred cells as well as at the entrance, exit, and sides of crossflow cells.[14] In fact, we could not fit the trends in Figures 2-3 and S8 using any single unstirred layer thickness. For example, a 10-μm unstirred layer gives K$^+$ passages that are much lower than the experimental data, whereas thicker unstirred layers give larger K$^+$ passages, but they overestimate the Li$^+$ passages (see Figures S16 and S17). As a first approximation, we modelled the data in Figures 3-4 and S8 using a linear combination of membrane regions with 10-μm and 75-μm unstirred layers. A combination of 3% of the area with a 75-μm unstirred layer and 97% of the area with a 10-μm unstirred layer yields the trends in Figures 2-3 and S8. A more complicated distribution of unstirred layer thicknesses would fit the data better, but we do not have any experimental justification of a particular distribution.

Li$^+$ passages. In contrast to K$^+$, Li$^+$ passage generally increases with pressure in Figures 3-4 and S8. As pressure increases, the K$^+$ passage decreases (except at the highest pressures) and this leads to depletion of K$^+$ within the nanopore (blue profiles in Figure 6). With negligible anion concentrations in the pore, the sum of the K$^+$ and Li$^+$ concentrations should approximately equal the fixed charge "concentration". Thus, as the pressure increases and K$^+$ becomes more depleted within the nanopore, the Li$^+$ concentration must rise to electrically compensate the negative fixed charge (see the green profiles in Figure 6), so Li$^+$ passage should increase. The decrease in streaming potential due to CP also increases Li$^+$ passage by decreasing the magnitude of its electromigration velocity. (The supplementary information (Section S5.4) shows that even a 1% drop in streaming potential will double the Li$^+$ passage).

The simultaneous decrease in K$^+$ passage and increase in Li$^+$ passage in most of the pressure range in Figures 3-4 and S8 are very attractive. Essentially, this method can offer highly pure Li$^+$ product without sacrificing productivity (or the amount of product obtained). This is similar to reverse osmosis (RO, water/salt separation), where salt rejection and water flux both initially increase with increasing transmembrane pressure until CP becomes a problem.[15] However, the transport mechanism in this study is very different from that in RO (solution-diffusion without convection).[15]

In conclusion, flow through negatively charged track-etched membranes allows separation of the monovalent ions Li$^+$ and K$^+$ with simultaneous high selectivity and high Li$^+$ passage. Increasing the flow rate in these separations overcomes the selectivity/permeability trade-off, at least until strong concentration polarization appears. Fabrication of highly negatively charged membranes with pore diameters of a few nm and high porosity may allow separations at higher ionic strengths, which could prove useful in salt purification.

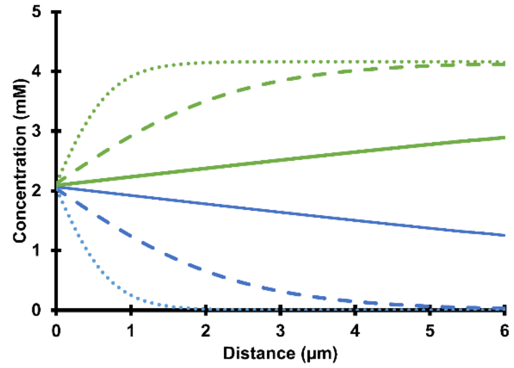

Figure 6. Simulated K$^+$ (blue) and Li$^+$ (green) concentration profiles for transport through track-etched membranes with a 10-μm unstirred layer. The figures show concentration profiles at various transmembrane pressures (single solid line = 0.7 bar; dashed line = 4.2 bar; dotted line = 13.8 bar). The feed contains a 0.1 mM LiCl, 0.1 mM KCl mixture, and the simulation assumes a pore diameter of 30 nm and a surface charge density of -3 mC/m^2.

The authors acknowledge funding from the Division of Chemical Sciences, Geosciences, and Biosciences, Office of Basic Energy Sciences of the U.S. Department of energy through Grant DE-SC0017618. AY thanks funding from the Spanish Ministry of Economy and Competitiveness through project CTM2017-85346-R. The authors also thank Center of Environmental Science & Technology, University of Notre Dame for sample analysis.

Conflicts of interest

There are no conflicts to declare.

Notes and references

1 (a) A. Razmjou, M. Asadnia, E. Hosseini, A. Habibnejad Korayem, and V. Chen, *Nat. Commun.,* **2019**, *10*, 5793; (b) J. M. Tarascon, and M. Armand, *Nature,* **2001**, *414*, 359-367.
2 D. S. Sholl, and R. P. Lively, *Nature,* **2016**, *532*, 435-437.
3 J.-C. G. Bünzli, and C. Piguet, *Chem. Soc. Rev.,* **2005**, *34*, 1048-1077.
4 H. Zhang, J. Hou, Y. Hu, P. Wang, R. Ou, L. Jiang, J. Z. Liu, B. D. Freeman, A. J. Hill, and H. Wang, *Sci. Adv.,* **2018**, *4*, eaaq0066.
5 (a) M. Kaganovich, W. Zhang, V. Freger, and R. Bernstein, *Water Res.,* **2019**, *161*, 381-391; (b) A. Szymczyk, and P. Fievet, *J. Membr. Sci.,* **2005**, *252*, 77-88.
6 (a) A. Esfandiar, B. Radha, F. C. Wang, Q. Yang, S. Hu, S. Garaj, R. R. Nair, A. K. Geim, and K. Gopinadhan, *Science,* **2017**, *358*, 511; (b) Y. Guo, Y. Ying, Y. Mao, X. Peng, and B. Chen, *Angew. Chem. Int. Ed.,* **2016**, *55*, 15120-15124; (c) K. Sint, B. Wang, and P. Král, *J. Am. Chem. Soc.,* **2008**, *130*, 16448-16449.
7 (a) E. Dražević, K. Košutić, and V. Freger, *Water Res.,* **2014**, *49*, 444-452; (b) G. M. Geise, H. B. Park, A. C. Sagle, B. D. Freeman, and J. E. McGrath, *J. Membr. Sci.,* **2011**, *369*, 130-138; (c) H. B. Park, J. Kamcev, L. M. Robeson, M. Elimelech, and B. D. Freeman, *Science,* **2017**, *356*, eaab0530.
8 E. Nightingale Jr, *J. Phys. Chem.,* **1959**, *63*, 1381-138.
9 P. Vanýsek, in *CRC Handbook of Chemistry and Physics, 100th Edition (Internet Version 2019)* (Ed.: J. R. Rumble), CRC Press/Taylor & Francis, Boca Raton, FL.
10 L. Dresner, *J. Phys. Chem.,* **1972**, *76*, 2256-2267.
11 (a) J. A. Armstrong, E. E. L. Bernal, A. Yaroshchuk, and M. L. Bruening, *Langmuir,* **2013**, *29*, 10287-10296; (b) C. Bardot, E. Gaubert, and A. E. Yaroshchuk, *J. Membr. Sci.,* **1995**, *103*, 11-17; (c) A. E. Yaroshchuk, *J. Membr. Sci.,* **2000**, *167*, 163-185.
12 (a) W. H. Keesom, R. L. Zelenka, and C. J. Radke, *J. Colloid Interface Sci.,* **1988**, *125*, 575-585; (b) I. H. Huisman, P. Prádanos, J. I. Calvo, and A. Hernández, *J. Membr. Sci.,* **2000**, *178*, 79-92.
13 A. Szymczyk, C. Labbez, P. Fievet, A. Vidonne, A. Foissy, and J. Pagetti, *Adv. Colloid Interface Sci.,* **2003**, *103*, 77-94.
14 (a) M. Fernández de Labastida, E. E. Licón, M. Bondarenko, and A. Yaroshchuk, *J. Membr. Sci.,* **2018**, *550*, 492-501; (b) A. Subramani, S. Kim, and E. M. V. Hoek, *J. Membr. Sci.,* **2006**, *277*, 7-17.
15 W. Zhou, and L. Song, *Environ. Sci. Technol.,* **2005**, *39*, 3382-3387.

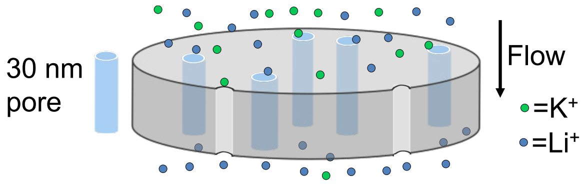

Flow through negatively charged pores yields highly selective passage of Li$^+$. Higher flow rate enhances both selectivity and Li$^+$ passage.